# Log-normal shadowing meets SINR: A numerical study of Capacity in Wireless Networks

Patrick Stuedi Gustavo Alonso
Department of Computer Science, ETH Zurich
8092 Zurich, Switzerland
Contact: stuedip@inf.ethz.ch

***Abstract*— The capacity of wireless multi-hop networks has been studied extensively in recent years. Most existing work tackles the problem from an asymptotic perspective and assumes a simplified physical layer model, as e.g., the protocol interference model or the path loss radio propagation. Real life network planning, provisioning and deployment can only be done with more precise statements about capacity in finite networks. With this in mind, we adopt a numerical approach based on Monte-Carlo methods to study capacity under various interference and radio propagation models, including the physical interference model and log-normal shadowing radio propagation. Our results indicate that, depending on the interference model, capacity may experience a three phase transition related to the connectivity of the network. We further show that throughput capacity increases in the presence of randomized radio propagation, even above the critical node density. Our analysis of the numerical data illustrates that log-normal shadowing creates more interference, but decreases the total amount of transmissions to be scheduled.**

## I. Introduction

Wireless multi-hop networks are often studied by choosing a network model that facilitates analytical treatment. In doing so, the problem is simplified by either making assumptions about the network, the radio propagation and/or the interference computation. One property of wireless multi-hop networks that has been studied extensively in this way is capacity. The main factor that limits capacity in wireless networks is interference, a consequence of using a shared communication medium. An accurate modeling of interference is fundamental in order to derive results of practical relevance. In the literature, two main interference models have been proposed [9]: the *protocol* and the *physical* interference model. In the *protocol* model, a transmission from a node $u$ is said to be received successfully by another node $v$ if no node $w$ closer to the destination node is transmitting simultaneously. However, in practice, nodes outside the interference range of a receiver might still cause enough cumulated interference to prevent the receiver from decoding a message from a given sender. This behavior is captured by the physical model, where a communication between nodes $u$ and $v$ is successful if the SINR (Signal to Interference and Noise Ratio) at $v$ (the receiver) is above a certain threshold. The physical model can also be less restrictive than the protocol model in a sense that a message from a node $u$ might be correctly received by node $v$ even if there is a simultaneously transmitting node $w$ close to $v$; for instance because $u$ is using a much larger transmission power than node $w$. Practical measurements have shown [1], [12], [26] that in some cases a node $v$ might also experience a stronger signal from a node $w$ farther away than another node $u$, even if both nodes $u$ and $w$ transmit at the same power level. Thus, similar to interference, an accurate modeling of signal propagation is fundamental when computing capacity in wireless networks. Unfortunately, the traditional path loss radio propagation model does not reflect reality accurately enough since the received signal strength is modeled as a direct function of the distance. A more sophisticated model for radio propagation is the log-normal shadowing radio propagation [18] where the signal strength perceived by a certain node not only depends on the distance between transmitter and receiver, but also includes some random factor. The log-normal shadowing radio propagation accounts for the fact that antennas are not perfectly isotropic, and, even more importantly, the environment might be obstructed by, e.g., buildings or trees. Analytical studies on capacity in the presence of realistic radio propagation and interference models – such as log-normal shadowing and physical interference – are difficult and we are not aware of any existing work. The simplified path loss radio propagation and the protocol interference model are most often used in theoretical studies. These studies typically derive bounds for throughput capacity as the

number of nodes in the network tends to infinity. In their seminal work, Gupta and Kumar demonstrated the existence of a global scheduling scheme achieving $\Omega(1/\sqrt{n \log n})$ for a uniform random network with a random traffic pattern [9]. It is not encouraging that the throughput available to each node approaches zero as the number of nodes increases. However, this analysis omits the constant factor that determines whether a realistic and finite network will have a useful per node throughput. While Gupta and Kumar's results illustrate an important property of wireless ad-hoc networks, more concrete statements about capacity in finite networks are necessary to support network planning and deployment. In this paper, we adopt a numerical approach to study capacity under various interference and radio propagation models, including the physical model and the log-normal shadowing radio propagation. In recent work [21], we have shown how the throughput capacity of a random network can be modeled as a random variable depending on the node distribution, the communication pattern, etc. A first contribution of this paper is to extend the model in [21] for different interference and radio propagation models. As in [21], we use Monte-Carlo methods to approximately compute expected values for throughput capacity under various parameter settings. Using the extended model, the paper makes the following additional contributions:

- The paper shows how throughput capacity behaves for different interference models. In particular, our results indicate that the capacity under the physical interference model, which is more realistic, is far less than the capacity under the protocol model, which is used in the majority of existing studies.

- The paper shows that, depending on the interference model, capacity experiences a three phase transition related to the connectivity of the network. In a first phase, the capacity is high but decreases to a minimum combined with a low network connectivity. In a second phase, while the network is in transition to become fully connected, capacity increases to reach a local maximum. In a third phase, the network is saturated and capacity drops with increasing network density.

- The paper demonstrates that throughput capacity increases as the effect of shadowing gets stronger. Our analysis illustrates that log-normal shadowing creates more interference, but decreases the total amount of transmissions to be scheduled. This is counterintuitive and very relevant for network provisioning.

## II. Network model and throughput capacity

In this section we extend the network model used in [21] by defining different interference and radio propagation models. Let $\mathcal{N}$ be the set of nodes in the network. We assume $(x_n, y_n) \in \mathcal{R}^2$ to be the coordinates of node $n$, identifying the node's position with respect to a rectangular area $\mathcal{A}$. We consider the set $\mathcal{N}$ of nodes to be uniformly distributed in $\mathcal{A}$. To avoid border effects we assume the rectangular area to be shaped as a torus. The distance between two nodes $n'$ and $n$ on a torus can be defined as

$$d(n', n) = \sqrt{(\frac{w}{2} - |\frac{w}{2} - \Delta x|)^2 + (\frac{h}{2} - |\frac{h}{2} - \Delta y|)^2}, \quad (1)$$

for $\Delta x = |x_n - x_n^{'}|$, $\Delta y = |y_n - y_n^{'}|$, and $w$ and $h$ as the weight and the height of rectangular area. Each node $n$ in the network is supposed to transmit with a signal power $P_n^{\mathrm{t}} \in [0, \infty[$. We use the tuple notation $(n^{'}, n)$ to refer to the transmission from a node $n^{'}$ to a node $n$. For a certain signal propagation function $\vartheta$, $P_{n \leftarrow n'} = \vartheta(P_{n'}^{\mathrm{t}}, d(n' - n)) \in [0, P_{n'}^{t}]$ denotes the power of the received signal at node $n$ due to the transmission $(n^{'}, n)$. In the simplest case, $\vartheta$ is a direct function of the distance. The path loss radio propagation model, for example, defines $\vartheta_{pl}(p, l) = p \cdot (l/l_0)^{-\rho}$ for some path loss exponent $\rho$, and $l_0$ as a reference distance for the antenna far-field. A more sophisticated model is the log-normal shadowing radio propagation [18]:

$$\vartheta_{sh}(p, l) = p \cdot (l/l_0)^{-\rho} \cdot 10^{X/10} \quad (2)$$

where $X$ is a gaussian random variable with zero mean and standard deviation $\sigma$ and $\rho$ is the aforementioned path loss exponent. In case of $\sigma$ equal 0, there is no random effect and $\vartheta_{sh} \equiv \vartheta_{pl}$. In this work, we assume the physical signal propagation to be symmetric. Thus, the gaussian random variable $X$ involved in the computation of $P_{n \leftarrow n'}$ is the same as the one involved in the computation of $P_{n' \leftarrow n}$[1]. From practical measurements, however, it is known that the signal strengths $P_{n \leftarrow n'}$ and $P_{n' \leftarrow n}$ corresponding to transmissions of two identical radio transmitters may not always be equal. This is due to tiny differences of the radio hardware and is taken into account in our model by the power distribution $P_n^{\mathrm{t}}$.

Whether a signal from a node $n'$ can be decoded correctly at node $n$ in the absence, or the presence, of concurrent transmissions, is determined by the interference model. In this work, we assume interference

[1]Therefore $P_n^{\mathrm{t}} \equiv P_{n'}^{\mathrm{t}} \Rightarrow P_{n \leftarrow n'} \equiv P_{n' \leftarrow n}$

models to be defined by a binary interference function $\kappa : \mathcal{N} \times \mathcal{N} \times \mathcal{P}(N) \longrightarrow \{0, 1\}$ with

$$\kappa(n^{'}, n, \mathcal{I}) = \begin{cases} 1 & \text{The signal of } n^{'} \text{ can be decoded at node } n \text{ under a set } \mathcal{I} \text{ of interferers} \\ 0 & \text{otherwise.} \end{cases} \tag{3}$$

The interference function for the protocol model [9] looks like

$$\kappa_{protocol}(n^{'}, n, \mathcal{I}) = 1 \Leftrightarrow d(n^{''}, n) > d(n', n), \forall n^{''} \in \mathcal{I} \tag{4}$$

and for the physical interference model [9] as follows:

$$\kappa_{sinr}(n^{'}, n, \mathcal{I}) = 1 \Leftrightarrow \frac{P_{n \leftarrow n^{'}}}{P_n^* + \sum_{n^{''} \in \mathcal{I}} P_{n \leftarrow n^{''}}} > \beta_{sinr} \tag{5}$$

for some threshold $\beta_{sinr}$ and $P_n^*$ as the thermal noise perceived at node $n$. Another interference model which is related to the CSMA/CA behavior of 802.11 is the disk interference model. Under disk interference,

$$\kappa_{disk}(n^{'}, n, \mathcal{I}) = 1 \Leftrightarrow d(n^{''}, n) > R_I, \forall n^{''} \in \mathcal{I} \tag{6}$$

where $R_I$ is called interference range. The disk model is often used in network simulators such as NS-2 [22]. Typical values for $R_I$ are in between $1.5$ and $2.5$ times the transmission range. We now assign two sets of nodes to each node $n \in \mathcal{N}$, namely $\mathcal{D}_n$ and $\mathcal{U}_n$.

$$\mathcal{D}_n = \{n^{'} \in \mathcal{N} \mid \kappa(n^{'}, n, \emptyset) = 1\} \tag{7}$$

is the set of nodes that can be correctly decoded at node $n$ in the absence of any other concurrent transmission.

$$\mathcal{U}_n = \{n^{'} \in \mathcal{D} \mid \kappa(n^{'}, n, I_{n^{'}}) = 1\} \tag{8}$$

contains all nodes $n^{'}$ that can be correctly decoded at node $n$ in the presence of a set of nodes $I_{n^{'}}$ transmitting concurrently as node $n^{'}$. For later use we define $\mathcal{D} = \{(n^{'}, n) \mid n^{'} \in \mathcal{D}_n, \forall n \in \mathcal{N}\}$ to be the set of transmissions in the network when interference is ignored, and $\mathcal{U} = \{(n^{'}, n) \mid n^{'} \in \mathcal{D}_n, \forall n \in \mathcal{N}\}$ to be the set of transmissions in the network if interference is considered.

## III. Scheduling Algorithms

Which transmissions in the network occur simultaneously is determined by the scheduling algorithm. In our model, we assume the medium to be divided into a set of channels $\psi_i$. Each channel can be seen as a set of directed transmissions $(n', n)$, with $n^{'} \in \mathcal{D}_n$, between two nodes $n'$ and $n$. Scheduling transmissions in multi-hop wireless networks so that no two transmission scheduled within the same channel interfere, is trivial for the protocol and the disk model, but turns out to be more difficult under the physical interference model. In general, the problem of scheduling is related to the traditional graph coloring problem, except that the vertices in the graph to be colored refer to the transmissions in the network and the edges in the graph refer to the interference conflicts. Two vertices conflict if their corresponding transmissions cannot be scheduled simultaneously. We call such a graph a *conflict graph*.

### A. Protocol model

For the protocol model, building a conflict graph is straightforward as shown in Algorithm 1. A conflict between two transmissions $(n', n)$, $(n^{'''}, n^{''})$ exists whenever either $d(n^{'''}, n) < d(n^{'}, n)$ or $d(n^{'}, n^{''}) < d(n^{'''}, n^{''})$, where $d(\cdot)$ is the distance function (Equation 1). Conflict graph construction and channel assignment under the protocol model are illustrated in Figure 1 for a small set of nodes.

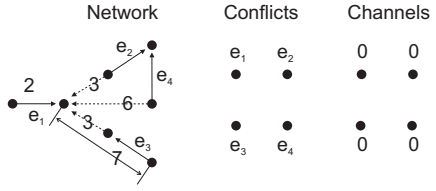


Fig. 1. Channel assignment under protocol interference. The straight line arrows represent the transmissions. The numbers assigned to the arrows refer to the distance the two corresponding nodes are apart. There is no conflict between any transmission and $e_1$ since all other nodes are farther apart (Algorithm 1). Note that both conflict graph and channel assignment are considered as temporary snapshots from the perspective of $e_1$

**Algorithm 1** Conflict graph under protocol interference

Input: Set of all transmissions $\mathcal{D}$
Output: Set of conflicts $\mathcal{C} \subseteq \{(e, e^{'}) \mid e, e^{'} \in \mathcal{D}\}$

```
C := ∅;
for all e := (n', n) ∈ D do
    for all n'' ∈ N \ {n, n'} do
        if d(n'', n) ≤ d(n', n) then
            Q := {(n''', n'') | n'' ∈ D_{n'''}}
            for all e' ∈ Q do
                C := C ∪ {(e', e), (e, e')};
            end for
        end if
    end for
end for
```

### B. Disk model

The procedure is similar in the disk model (Algorithm 2), where a conflict between two transmissions $(n', n)$, $(n^{'''}, n^{''})$ exists whenever either $d(n^{'''}, n) < R_I$ or $d(n^{''}, n^{'}) < R_I$, where $R_I$ is the interference range. An example of a conflict graph and channel assignment under disk interference is given in Figure 2.

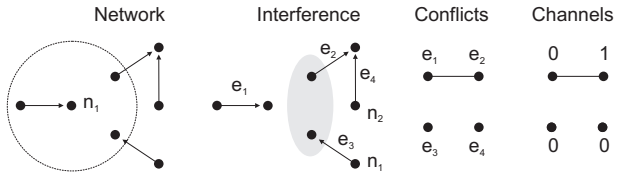


Fig. 2. Channel assignment under physical interference. The straight line arrows represent the transmissions. The disk centered at node $n_1$ refers to the interference range with radius $R_I$, compliant with Equation 6. According to Algorithm 2, nodes in the grey area are considered as interfering nodes. Transmissions $e_3$ and $e_4$ do not conflict with $e_1$ because node $n_1$ and $n_2$ are not included in the grey area. Note that both conflict graph and channel assignment are considered as snapshots from the perspective of $e_1$

**Algorithm 2** Conflict graph under disk interference

Input: Set of all transmission $\mathcal{D}$, interference range $R_I$
Output: Set of conflicts $\mathcal{C} \subseteq \{(e, e^{'}) \mid e, e^{'} \in \mathcal{D}\}$

$\mathcal{C} := \emptyset$;
**for all** $e := (n^{'}, n) \in \mathcal{D}$ **do**
  **for all** $n^{''} \in \mathcal{N} \backslash \{n, n^{'}\}$ **do**
    **if** $d(n^{''}, n) \leq R_I$ **then**
      $\mathcal{Q} := \{(n^{''}, n^{'''}) \mid n^{''} \in \mathcal{D}_{n^{'''}}\}$
      **for all** $e^{'} \in \mathcal{Q}$ **do**
        $\mathcal{C} := \mathcal{C} \cup \{(e^{'}, e), (e, e^{'})\}$;
      **end for**
    **end if**
  **end for**
**end for**

### C. Physical model

In the physical model, conflicts between two transmissions cannot be determined without considering all other transmissions. As an example, two nodes in distance $2d$ may interfere with a transmission at distance $d$ if their interference is accumulated. For a node $n^{'}$ to belong to $\mathcal{U}_n$, $\kappa_{physical}(n^{'}, n, \mathcal{N} \setminus \mathcal{C}_{n \leftarrow n^{'}})$ must compute to 1, given $\mathcal{C}_{n \leftarrow n^{'}}$ contains all nodes $n^{''}$ acting as a sender in a transmission that conflicts with the transmission $(n^{'}, n)$.

In practice, of course, one wants to find the minimum set $\mathcal{C}_{n \leftarrow n^{'}}$ of conflicts for a transmission $(n^{'}, n)$, because this minimizes the number of channels to be used at a later point in time. How to compute the minimum set of conflicts for a given set of transmissions $\mathcal{D}$ in the physical interference model is shown in Algorithm 3. For a given transmission $(n^{'}, n)$, the algorithm operates by gradually testing the SINR ratio with an increasing set of interferers, starting with the node contributing the lowest signal power. At the point where the cumulated interference of a node $n^{''}$ leads to a SINR ratio smaller than $\beta_{sinr}$, all transmitting nodes $n^{'''}$ with $P_{n \leftarrow n^{'''}} \geq P_{n \leftarrow n^{''}}$ are considered as interferers and their associated transmissions are defined as conflicts with $(n^{'}, n)$.

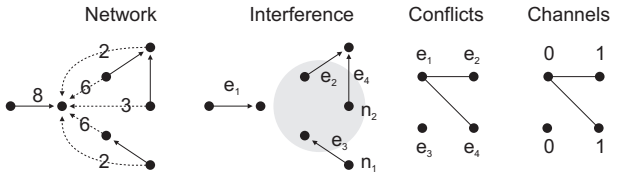


Fig. 3. Channel assignment under physical interference. The straight line arrows represent the transmissions. The dotted arrows denote signals which contribute to the interference noise of transmission $e_1$. The weight assigned to an edge corresponds the signal strength. We assume the thermal noise $P^*$ and $\beta_{sinr}$ used in Equation 5 to be 1. According to Algorithm 3, nodes in the grey area are considered as the smallest set of nodes such that the remaining cumulated interference does not prohibit transmission $e_1$ to be established. There is no conflict between transmissions $e_1$ and $e_3$ because node $n_1$ is not included in the grey area. Note that both conflict graph and channel assignment are considered as snapshots from the perspective of $e_1$

**Algorithm 3** Conflict graph under physical interference

Input: Set of all transmission $\mathcal{D}$
Output: Set of conflicts $\mathcal{C} \subseteq \{(e, e^{'}) \mid e, e^{'} \in \mathcal{D}\}$

$\mathcal{C} := \emptyset$;
**for all** $e := (n^{'}, n) \in \mathcal{D}$ **do**
  L := sort($\mathcal{N} \backslash \{n^{'}, n\}$) such that $n^{''} \prec n^{'''} \longleftrightarrow P_{n \leftarrow n^{''}} < P_{n \leftarrow n^{'''}}$
  $\mathcal{M}^* := \emptyset$;
  **for all** $n^{''} \in L$ **do**
    $\mathcal{M}^* := \mathcal{M}^* \cup \{n^{''}\}$
    **if** $\kappa_{sinr}(n^{'}, n, \mathcal{M}^*) = 0$ **then**
      $\mathcal{Q} := \{(n^{''}, n^{'''}) \mid n^{''} \in \mathcal{D}_{n^{'''}}\}$
      **for all** $e^{'} \in \mathcal{Q}$ **do**
        $\mathcal{C} := \mathcal{C} \cup \{(e^{'}, e), (e, e^{'})\}$;
      **end for**
    **end if**
  **end for**
**end for**

We have shown how a conflict graph can be built for the different interference models. Based on the conflict graph, efficient coloring algorithms might be used to assign channels to the transmissions (represented as nodes in the conflict graph). Finding the minimum number of channels, however, is an NP hard problem

and thus is not feasible for large networks [13], [17]. We decided to apply a *Greedy* channel assignment algorithm (Algorithm 4). Algorithm 4 assigns channels to transmissions in a greedy way, so that no two transmission $e_1$, $e_2$ will be scheduled using the same channel if there exists a conflict between the two transmissions ($(e_1, e_2) \in \mathcal{C}$). Algorithm 4 further assigns channels in a traffic proportional way, meaning that each node pair $(n^{'}, n)$, with $n^{'} \in \mathcal{D}_n$, is assigned exactly as many channels as there are flows occupying the wireless link. Conflict graph and channel assignment for the physical interference model are illustrated in Figure 3 in a small example network.

**Algorithm 4** $Greedy$ channel assignment

Input: Set of all transmission $\mathcal{D}$, set of conflicts $\mathcal{C}$
Output: Set of channels $\{\psi_0, \psi_1, ..., \psi_{T-1}\}$ with $\psi_i \subseteq \mathcal{D}$

**for all** $e \in \mathcal{D}$ **do**
  **for** $i := 0$; $i < \mu(e)$ **do**
    $\mathcal{Q} := \{e^{'} \mid (e, e^{'}) \in \mathcal{C}\}$
    $\Omega := \emptyset$;
    **for all** $e^{'} \in \mathcal{Q}$ **do**
      $\Omega := \Omega \cup \{\psi_i \mid e^{'} \in \psi_i\}$
    **end for**
    $\psi_i := freechannel(\Omega)$;
    $\psi_i := \psi_i \cup \{e\}$;
  **end for**
**end for**

**freechannel(**$\mathcal{Q}$)
$\Omega^* := sort(\mathcal{Q})$ such that $\psi_i \prec \psi_j \longleftrightarrow id(\psi_i) < id(\psi_j)$
$i := -1$
**for all** $\psi \in \Omega$ **do**
  **if** $id(\psi) > i + 1$ **then**
    **break;**
  **end if**
  $i := id(\psi)$;
**end for**
**return** $\psi_{i+1}$;

### D. Schedule graph

Coming back to the definition of $\mathcal{U}_n$, we can say, a node $n^{'}$ belongs to $\mathcal{U}_n$ if $I_{n^{'}}$ in Equation 8 is defined as the set of nodes transmitting in the same channel as node $n^{'}$. Given a schedule and the set $\mathcal{U}_n$ for each node, we define a so called schedule graph as a directed and weighted graph $G_T(\mathcal{N}, \mathcal{E})$, where $\mathcal{E}$ denotes the set of directed edges with

$$\mathcal{E} = \{(n^{'}, n) \in \mathcal{N} \times \mathcal{N} \mid n^{'} \in \mathcal{U}_n \wedge n \in \mathcal{D}_{n^{'}}\}. \quad (9)$$

The set $\mathcal{E}$ includes all transmissions $(n^{'}, n)$ whose signals can be decoded correctly at node $n$ under interference, while the reverse signal might only be correctly decoded if there is no interference. Note that Equation 9 models the acknowledgment as an infinite small packet not occupying the medium. The subscript $T$ indicates the number of channels used (Algorithm 4). In [21], we have shown that the throughput capacity per node, for a given schedule graph $G_T(\mathcal{N}, \mathcal{E})$ and a given traffic pattern $\Upsilon \subseteq \{(n^{'}, n) \in \mathcal{N} \times \mathcal{N} | n^{'} \neq n\}$, computes as

$$\zeta = \frac{1}{|\Upsilon|} \sum_{(n^{'}, n) \in \Upsilon} \frac{W \cdot B_{n^{'}, n}}{T}, \quad (10)$$

where $W$ is the maximum transmission rate equal to all nodes, $T$ is the number of channels used in total, and $B_{n^{'},n}$ indicates the lowest capacity per link available between two nodes along the path from $n^{'}$ to $n$. The capacity per link itself corresponds to the number of channels assigned to that link divided by the number of flows sharing the link. In [21], we also show that

$$\frac{1}{|\Upsilon|} \sum_{(n^{'''}, n^{''}) \in \Upsilon} \frac{1}{k} \sum_{i=0}^{k-1} \zeta_{n^{'''}, n^{''}}|_{X = X_i^*} \quad (11)$$

can be used to approximately compute the expected value of $\zeta$ for a given set of parameters by sampling over $k$ realizations of the underlying random network, with $X_i^*$ as a concrete set of node placements in the area $\mathcal{A}$. In this paper, we make use of Equation 11 and refer to [21] for further details on how to derive it.

## IV. Path loss radio propagation

### A. Network settings

We first study capacity under different interference models using path loss radio propagation and look at effects of log-normal shadowing radio propagation on capacity in the second part of the paper (Section V). The network configuration we consider consists of 20 to 500 nodes uniformly distributed on a torus of size $2000 \times 2000m^2$. For the physical interference model, we use a threshold $\beta_{sinr}$ of 4 decibel, which is the lowest tolerable threshold of an Orinocco PCMCIA Silver/Gold wireless network card so that it can still function at a rate of 1Mbps. The transmission power for every node is kept constant and the thermal noise $P^*$ is adjusted such that the resulting transmission range becomes $200m^2$. We use Equation 11 with a sample size $k$ of 1000 to compute the capacity of the network. A random traffic pattern with $|\mathcal{N}|$ flows is considered, where each node is the originator of a flow to a randomly chosen destination, and a shortest path routing is adopted. Capacity in the sense of Equation 11 is meant to be the average capacity among all flows, which for a sufficiently high sample size

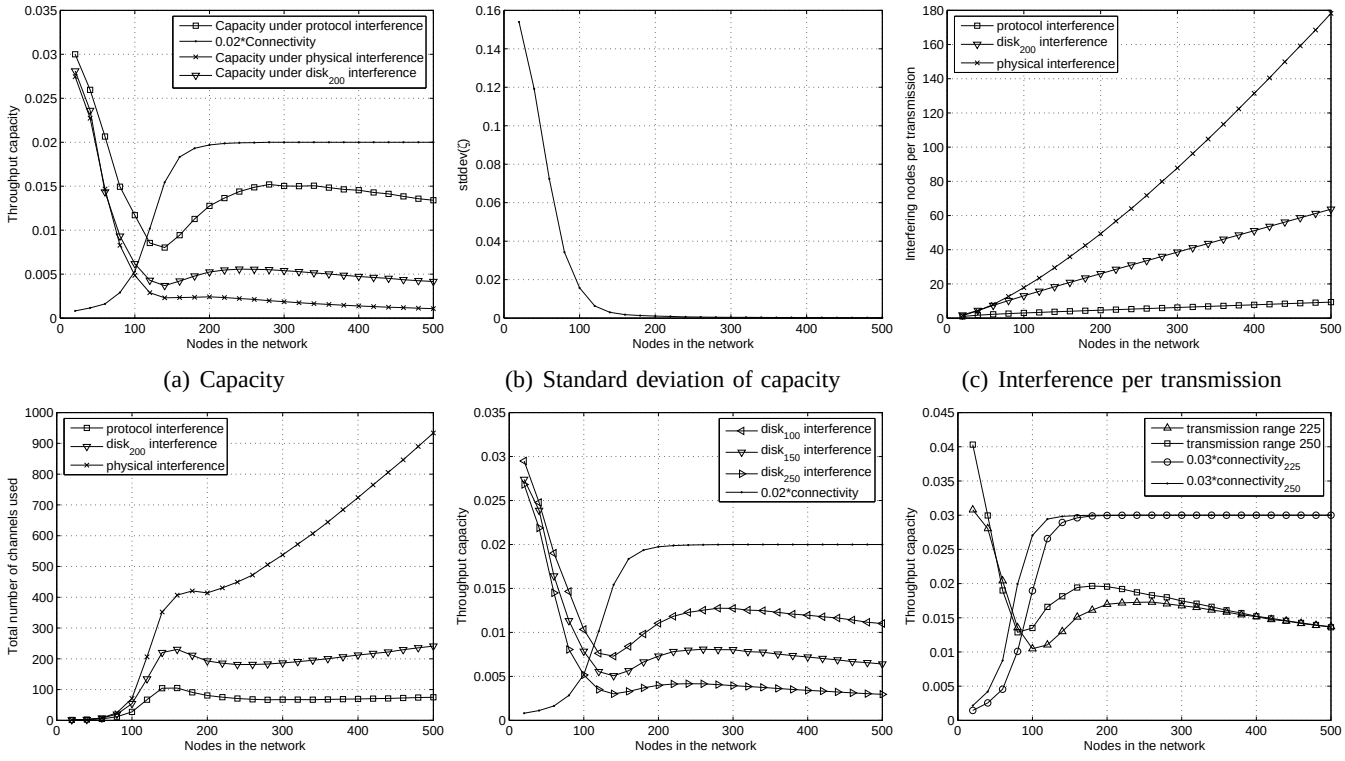


(a) Capacity (b) Standard deviation of capacity (c) Interference per transmission

(d) Total number of channels (e) Disk model for different $R_I$ values (f) 3-phase transition in the protocol model

Fig. 4. Capacity under different interference models using path loss radio propagation

is a very good approximation for the expected capacity per node [21]. In the following section, we illustrate how capacity, the number of channels used or the number of interferers per transmission, evolve as the network density increases. Throughout the paper, the term $disk_z$ refers to the disk interference model with $R_I = z$.

### *B. Capacity Analysis*

Figure 4a shows the capacity of each of the three interference models, protocol, disk and physical, and relates the result to the connectivity of the network. Connectivity is scaled with a factor of $0.02$ to facilitate the comparison. First, Figure 4a clearly shows the gap between the protocol model, which is most commonly used in theoretical work, and the physical model, which is supposed to be a more accurate description of a real network. The result contradicts the work in [5], where it is suggested that the physical interference model may increase the network capacity compared to the protocol model. In fact, already for a SINR threshold of only 4 decibel and pathloss $\rho$ of 3, the number of interferers per transmission (Figure 4c), and thus also the number of channels (Figure 4d) needed, is much higher in the physical model than under the protocol model. To illustrate how an increasing set of interfering nodes affects capacity, we have computed capacity under the disk interference model, with an interference range increasing from $100m$ to $250m$ (remember that the transmission range is $200m$). Figure 4e shows that an interference factor of 2.5 results in a throughput capacity comparable to the one in the physical model with $\beta_{sinr} = 4dB$.

The common behavior under all three interference models is that the capacity is high when the network density is low and drops when the network density becomes high. This is the expected behavior since additional nodes introduce more interference and diminish capacity. The high capacity in the beginning might still be surprising since the network is hardly connected with less than 100 nodes. However, by looking at the numerical data in more detail, we found that in the case of low network density, few flows have a very high throughput due to the low interference and the short hop distances. The capacity of these flows compensates the fact that most of the other flows do not even have connectivity and therefore also no capacity. Obviously, although throughput capacity reaches its maximum with a low network density, network planners may not want to consider such settings as practical, since the capacity is distributed very unevenly. This is illustrated in Figure

4b that shows the standard deviation of the computed capacity for the protocol model. A similar result can be obtained for both the disk and the physical interference model.

### C. Three phase transition

Another interesting observation from Figure 4a is that not only is there a gap between the capacity under the physical and the protocol model, but the shape of the curve in the protocol model also differs from the one in the physical model in as it follows an additional transition when the network contains around 200 nodes. While the capacity under physical interference drops almost monotonically, the capacity under the protocol interference has a local maximum right after the network becomes fully connected. To illustrate this behavior, we have computed the throughput capacity for the very same configuration as for Figure 4a, but once with a transmission power resulting in a 225 $m^2$ transmission range and once with a transmission power resulting in a 250 $m^2$ transmission range (Figure 4f). In both cases, the capacity of the network increases directly after the network reaches a connectivity of approximately $80\%$. The correlation between capacity and connectivity is obvious, since the higher the network connectivity, the more flows find their route to the destination, contributing to the average capacity of the network (Equation 11). However, high connectivity is achieved by adding more nodes to the network which creates more interference. In the end, it depends on the interference model whether the capacity improvement through more successful flows may compensate the additional interference created by adding more nodes. In the physical interference model, since the number of interfering nodes per transmission is high (Figure 4c), having a greater number of successful flows rarely helps. In the protocol, and up to some point also in the disk interference model, since the number of interfering nodes per transmission is relatively low, having more successful flows might help to improve the capacity. At some point, the network is connected and adding more nodes does not lead to more successful flows, but only increases the interference. After the network density has reached this point, capacity under the protocol and the disk interference model also decrease. Considering the entire distribution of the capacity curve for the protocol model in Figure 4a, one can adhere that capacity experiences a three phase transition related to the connectivity of the network. In a first phase, where the network is rarely connected, adding additional nodes to the network lowers the network capacity since the common media has to be shared by more nodes. In a second phase, adding more nodes to the network increases capacity because more flows find their route to the destination. In a third phase, however, the interference generated by the additional nodes becomes too strong and the network capacity decreases again.

As a summary, already under the simplified path loss radio propagation, the throughput capacity behaves quite differently in the various interference models. The difference is not only in the absolute value of capacity, but also in the shape of the capacity curve as the node density increases. It emerges that the interdependency between the number of flows that can successfully be scheduled (which increase with increasing node density) and the amount of interference perceived per transmission (which decrease with increasing node density) decides whether for a given interference model capacity is monotonically decreasing or has a local maximum at the connectivity transition phase.

## V. Effects of log-normal shadowing

We now consider a more accurate radio propagation model. The log-normal shadowing radio propagating, as opposed to the path loss model, captures effects caused by imperfect antennas and environmental obstructions. The *shadowing deviation* $\sigma$ in $\vartheta_{sh}$ (Equation 2) can be seen as a measure of radio propagation irregularity. Please note that in the case of $\sigma = 0$, the log-normal shadowing model is identical to the path loss model used in Section IV. The network configuration for this section corresponds to the settings used in Section IV.

### A. Shadowing under protocol interference

We first look at throughput capacity for different values of $\sigma$ in the protocol model. Similarly to what we did in Section IV, we relate the results obtained for capacity with results about network connectivity. It is known from [3] that network connectivity increases with increasing values of $\sigma$. This is mainly because the expected signal strength according to Equation 2 increases when $\sigma$ rises[2]. Considering the relation between connectivity and capacity as pointed out in Section IV, one might suggest that capacity also increases with increasing $\sigma$, at least during the connectivity transition phase. On the other hand, since the expected signal strength at a given distance also grows with $\sigma$, the interference per link, perceived due to transmissions of other nodes, might increase and

[2]The expected signal strength received at distance r can be computed as follows: $p_r = p_t \left(\frac{r}{d_0}\right)^{-\rho} \exp\left(\frac{\log(10)^2}{200}\sigma^2\right)$

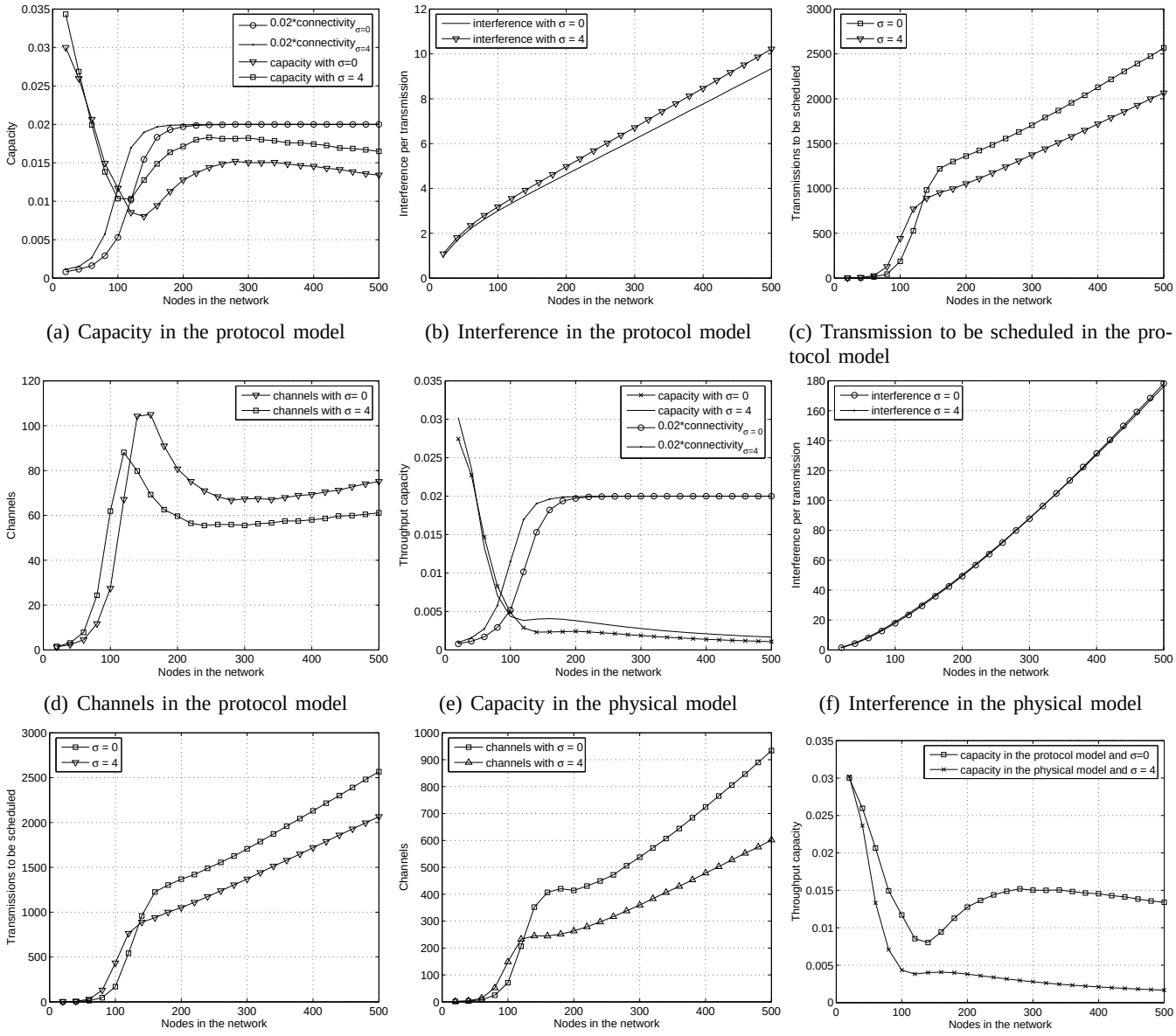


(a) Capacity in the protocol model

(b) Interference in the protocol model

(c) Transmission to be scheduled in the protocol model

(d) Channels in the protocol model

(e) Capacity in the physical model

(f) Interference in the physical model

(g) Transmission to be scheduled in the physical model

(h) Channels in the physical model

(i) Pathloss/protocol model vs. shadowing/physical model

Fig. 5. Effects of log-normal shadowing radio propagation for both protocol and physical interference

diminish capacity. Figure 5a illustrates that as a matter of fact the first argument holds, and capacity does grow with increasing value of $\sigma$. The interesting aspect here is that capacity for $\sigma = 4$ not only exceeds capacity for $\sigma = 0$ during the connectivity transition phase, but also above the critical node density (which is about 200 nodes in our example). This is surprising because the number of interfering nodes per transmission indeed grows (Figure 5b) as effects of shadowing take place. The reason why shadowing still leads to a higher capacity, even above the critical density, becomes clear when considering the total number of transmissions that need to be scheduled for a given scenario. Figure 5c shows that for a $\sigma = 4$, less transmissions need to be scheduled than for a $\sigma = 0$, requiring less channels in total. This makes sense since shadowing not only increases the average signal strength at a given distance, but also leads to a larger transmission range, and it thus decreases the number of hops needed between source and destination node. It becomes evident that the reduction in transmissions compensates the fact that shadowing creates more interference which in turn leads to a capacity increase. This is an important result

when considering provisioning in real networks.

An interesting behavior can be observed in Figure 5d. While the number of channels for $\sigma = 4$ is below the curve for $\sigma = 0$ as soon as the network density exceeds the critical node density, the opposite is true when the network is only partially connected. Obviously, during the first phase, the number of channels is determined by the increase in connectivity where more flows need to be scheduled and thus more channels are needed. During the second phase, the total amount of transmissions, which decreases as $\sigma$ grows, becomes the dominant factor.

### *B. Shadowing under physical interference*

Considering capacity under the physical interference model, a similar result as for the protocol model can be observed in Figure 5e. Again, shadowing increases capacity, even though the scaling of the y-axis and the absolute values for capacity in Figure 5e makes it appear less dramatic. As in the protocol model, less transmission need to be scheduled (Figure 5g) in the presence of shadowing and therefore also less channels are used (Figure 5h). Note that since Algorithm 4 produces a conflict free channel assignment, the amount of transmissions to be scheduled does not depend on the interference model. The physical model differs from the protocol model in the fact that there is no difference in the number of interferers per transmission for $\sigma = 0$ and $\sigma = 4$ (Figure 5f). This is a result of Algorithm 3 which finds an equal size minimum set of interferers, independent of the shadowing deviation used for signal propagation.

As a summary, the results show that throughput capacity increases as the effect of shadowing becomes stronger. This is mainly because shadowing creates more interference, but at the same time decreases the total amount of transmissions to be scheduled. A realistic model of a wireless multi-hop network may combine physical interference with log-normal radio propagation. In view of this (Figure 5i), some of the conclusions derived from existing work based on the protocol [6], [9], [14], [10], [19], [15], [24], [8], [11] model will have to be revised to adjust them to the more accurate capacity calculations of above. With this work, we have illustrated how certain physical layer issues may affect throughput capacity, not only in a sense of absolute values but also in its behavior as the node density increases.

## VI. Related Work

Capacity and scheduling issues have been in the focus of research for many years [9], [7], [14]. In contrast to the consensus that accurate physical layer models are important, many recent studies are still based on a simplified interference model, such as the protocol or the disk model. In [6] the authors use the protocol model to investigate the interaction between channel assignment and distributed scheduling in multi-channel multiradio wireless mesh networks. Broadcast capacity of multihop wireless networks under protocol interference is studied in [10]. The *k*-hop interference model is an extension to the traditional protocol model in that it considers all nodes within a hop distance of *k* from the receiver as interfering nodes. Such a model is studied in [19] to derive bounds for the scheduling complexity. The relation between the *k*-hop neighborhood and the set of interfering nodes, however, is not clear. An interference model similar to the disk model described in this work is used in [15]. The authors describe an improved packet scheduling algorithm based on virtual coordinates. In [24], the authors also use a disk based interference model but their work allows for different transmission and interference range settings per node. Effects of variable transmission power have also been studied earlier by [8]. A throughput optimal adjustment of the carrier sense threshold (which determines the interference range of a node) is proposed in [11]. The need for more accurate physical layer models has been recognized in [2], where the authors propose Algorithms to improve delay and throughput performance under the physical interference model and Rayleigh fading [18]. Joint congestion control and resource allocation, also under physical interference, has been investigated in [20]. One of the first approaches to apply combined topology control and channel assignment algorithms to SINR-based interference models in multi-hop wireless networks can be found in [16]. A fast scheduling algorithm for the physical interference model is proposed in [5]. However, all these studies are based on radio propagation models in which the received signal strength is determined as a direct function of the distance between transmitter and receiver. There is some work on the effect of log-normal shadowing on connectivity [3]. Effects of shadowed radio propagation on capacity have also been analyzed [27] but without considering multihop networks. An asymptotic analysis of capacity in the presence of fading including wireless multihop networks is given in [25]. While asymptotic bounds certainly indicate the generic behavior of ad hoc networks for large number of nodes, they do not give any information on concrete throughput capacity and small networks. Recently, there has been some effort to compute concrete throughput values [4], [23] using integer linear programming (*ILP*). However, *ILP* makes

it very difficult to model physical network properties, hence, most of these studies are based on a simplified network model.

## VII. Conclusions

In this paper, we adopt a numerical approach to studying throughput capacity of finite wireless multihop networks under log-normal radio propagation and physical interference. The results provided contrast in many aspects with a large amount of work studying capacity from an asymptotic perspective using simplified physical layer models. Our results illustrate that there is a significant performance gap between capacity under the physical interference model and capacity under the most commonly used protocol model. This is of particular interest since the physical model is supposed to reflect effective interference much more accurately than the protocol model. In our paper, we further show that, depending on the interference model, capacity may experience a three phase transition related to the connectivity of the network. In a first phase, where the network is rarely connected, adding additional nodes to the network may decrease the network capacity since the common media has to be shared by more nodes. In a second phase, adding more nodes to the network may increase capacity because more flows find their route to the destination. In a third phase, however, the interference generated by the additional nodes becomes too strong and the network capacity drops again. In this paper, we also show that throughput increases in the presence of randomized radio propagation, even above the critical node density. Our results illustrate that log-normal shadowing does create more interference but also decreases the total amount of transmissions to be scheduled.

## References


[1] D. Aguayo and J. Bicket et al. Link-level measurements from an 802.11b mesh network. SIGCOMM, 2004.

[2] A. Bader and E. Ekici. Throughput and delay optimization in interference-limited multihop networks. In *MobiHoc '06*. ACM Press, 2006.

[3] C. Bettstetter and C. Hartmann. Connectivity of wireless multihop networks in a shadow fading environment. In *MSWIM '03*. ACM Press, 2003.

[4] P. Bjorklund, P. Varbrand, and D. Yuan. Resource optimization of spatial tdma in ad hoc radio networks: A column generation approach. IEEE INFOCOM, March 2003.

[5] G. Brar, D. M. Blough, and P. Santi. Computationally efficient scheduling with the physical interference model for throughput improvement in wireless mesh networks. In *MobiCom '06*. ACM Press, 2006.

[6] A. Brzezinski, G. Zussman, and E. Modiano. Enabling distributed throughput maximization in wireless mesh networks: a partitioning approach. In *MobiCom '06*, 2006.

[7] O. Dousse and P. Thiran. Connectivity vs capacity in dense ad hoc networks. In *IEEE INFOCOM, Hong Kong, 2004.*, 2004.

[8] J. Gomez and A. Campbell. A case for variable-range transmission power control in wireless ad hoc networks. IEEE INFOCOM, March 2004.

[9] P. Gupta and P. Kumar. Capacity of wireless networks. *Information Theory*, 46(2):388–404, 2000.

[10] A. Keshavarz-Haddad, V. Ribeiro, and R. Riedi. Broadcast capacity in multihop wireless networks. In *MobiCom '06*. ACM Press, 2006.

[11] T.-S. Kim, J. C. Hou, and H. Lim. Improving spatial reuse through tuning transmit power, carrier sense threshold, and data rate in multihop wireless networks. In *MobiCom '06*. ACM Press, 2006.

[12] D. Kotz, C. Newport, R. S. Gray, J. Liu, Y. Yuan, and C. Elliott. Experimental evaluation of wireless simulation assumptions. In *MSWiM '04*. ACM Press, 2004.

[13] S. Krumke and M. Marathe. Models and approximation algorithms for channel assignment in radio networks. *Wirel. Netw.*, 7(6):575–584, 2001.

[14] P. Kyasanur and N. H. Vaidya. Capacity of multi-channel wireless networks: impact of number of channels and interfaces. In *MobiCom '05*. ACM Press, 2005.

[15] H. Lim, C. Lim, and J. C. Hou. A coordinate-based approach for exploiting temporal-spatial diversity in wireless mesh networks. In *MobiCom '06*. ACM Press, 2006.

[16] T. Moscibroda, R. Wattenhofer, and A. Zollinger. Topology control meets SINR: the scheduling complexity of arbitrary topologies. In *MobiHoc '06*, 2006.

[17] S. Ramanathan and E. L. Lloyd. Scheduling algorithms for multihop radio networks. *IEEE/ACM Trans. Netw.*, 1(2):166–177, 1993.

[18] T. S. Rappaport. *Wireless Communications: Principles & Practice*. Prentice Hall, 2002.

[19] G. Sharma, R. R. Mazumdar, and N. B. Shroff. On the complexity of scheduling in wireless networks. In *MobiCom '06*, 2006.

[20] P. Soldati, B. Johansson, and M. Johansson. Proportionally fair allocation of end-to-end bandwidth in stdma wireless networks. In *MobiHoc '06*, 2006.

[21] P. Stuedi and G. Alonso. Computing throughput capacity for realistic wireless multihop networks. In *MSWiM '06*. ACM Press, 2006.

[22] The VINT Project. The NS network simulator.

[23] S. Toumpis and A. Goldsmith. Capacity regions for wireless adhoc networks. *Transactions on Wireless Communications*, 2:736–748, 2003.

[24] W. Wang, X.-Y. Li, O. Frieder, Y. Wang, and W.-Z. Song. Efficient interference-aware tdma link scheduling for static wireless networks. In *MobiCom '06: Proceedings of the 12th annual international conference on Mobile computing and networking*. ACM Press, 2006.

[25] F. Xue, L.-L. Xie, and P. R. Kumar. The transport capacity of wireless networks over fading channels. *IEEE Transactions on Information Theory*, 51(3):834–847, 2005.

[26] G. Zhou, T. He, S. Krishnamurthy, and J. A. Stankovic. Impact of radio irregularity on wireless sensor networks. In *MobiSys '04*. ACM Press, 2004.

[27] M. Zorzi and S. Pupolin. Optimum transmission ranges in multihop packet radio networks in the presence of fading. *IEEE Trans. On Communication*, 43(7), July 1995.